Supplementary Material

Real-Time Monitoring of the Sialic acid Biosynthesis Pathway by NMR

Jacob L. Gorenflos López[ab], Peter Schmieder[a], Kristin Kemnitz-Hassanin[a], Hatice Ceyda Asikoglu[ac], Arif Celik[ab], Christian Stieger[ab], Dorothea Fiedler[ab], Stephan Hinderlich[c] and Christian P.R. Hackenberger[ab]

[a]Leibniz-Institut für Molekulare Pharmakologie, Robert-Roessle-Strasse 10, 13125 Berlin, Germany. Email: hackenbe@fmp-berlin.de
[b]Humboldt Universität zu Berlin, Department Chemie, Brook-Taylor-Strasse 2, 12489
[c]Berliner Hochschule für Technik, Department Life Sciences & Technology, Seestrasse 64, 13347 Berlin, Germany.

Content

1 Experimental

1.1 Real-time NMR Assay with recombinant enzymes and in cytosolic extract

1.1.1 Experimental set-up

NMR spectra were recorded at 295 K at 600 MHz (^{1}H frequency) on Bruker AV-III spectrometers (Bruker Biospin, Rheinstetten, Germany) using a cryogenically cooled 5 mm QCI-triple resonance probe equipped with a one-axis self-shielded gradient system. Samples were stored during the experiments in a SampleCase™ Cooled sample changer, which kept the temperature of the samples at 295 K as well. The software used to control the spectrometer was topspin 3.5 pl6. Temperature had been calibrated using d_4-methanol.
Experiments with recombinant enzymes and in cytosolic extract were conducted with the same set-ups, NMR methods and analysis. They only differed in the one buffer component:
1) Experiments with recombinant enzymes were conducted with 0.05% w/v BSA (freshly prepared for every experiment using 10% BSA stock solutions stored in aliquots at -20 °C).
2) Experiments with cytosolic extract were conducted with 1 pill per 10 mL of the cOmplete™, EDTA-free Protease Inhibitor Cocktail by Roche. These could be stored for up to one week at 4 °C without affecting experimental outcomes.

The pH of ATP and PEP stock solution has to be adjusted. 1 M ATP stocks were used. PEP was found to be soluble up to roughly 0.5 M. Carbohydrates were diluted to 10 mM stock solutions. If not indicated differently, experiments were conducted in buffer containing 100 mM HEPES, 100 mM NaCl, 10 mM $MgCl_2$, pH 7.5. The substrates, cofactors, intermediates, and inhibitors of the sialic acid biosynthesis pathway were diluted in reaction buffer to their final 2x concentrations. Recombinant enzymes or cytosolic extract were also diluted in reaction buffer to their final 2x concentrations. 10% of one of these cocktails was set up to be D_2O. This depended on the experimental set-up and was adjusted to always reduce pipetting steps. The reactions were started by mixing the two aforementioned 2x solutions to a final volume of 600 µL and transferring this reaction cocktail to an NMR tube. The sample holder and the spectrometer were set the same temperature if the sample temperature was 295 K. Reaction kinetics were slow at this temperature and samples were shuttled between the NMR spectrometer and the sample holder. Experiments used different measuring intervals. In this study, the most experiments recorded in 1 h was 12, which was repeated up to 20 times
A specific number of experiments in regularly interspaced intervals with a defined start time was set up. The specified start time allowed to pre-mix the reaction components at a pre-defined time point, ensuring consistent reactions throughout experiments. In this study, all reactions were started 2 min before the time point zero measurements. To ensure that all experiments fit in their allotted time frame, extensive experiments were conducted for each method, testing the speed at which samples are processed once they are placed in the sample holder. Several standard configurations were set to speed up the pre-acquisition time. Temperature handling was turned off, which necessitated the same temperature for the pre-mixed sample, the sample holder, and the sample temperature – if this requirement is not met, signals became most inconsistent throughout an experiment. Shimming standard gradient shimming was performed right after sample insertion. Tuning and matching were turned off for all experiments. Acquisition parameters were optimised for all experiments to run as efficiently as possible to separate the peaks of the intermediates in the sialic acid biosynthesis pathway. This was achieved by reducing the number of scans, the spectral width of the second dimension in 2D NMR spectra - to solely include the peaks of interest - and non-uniform sampling.
The number of dummy scans was reduced to 2, and P1 pulses were determined for all used buffer systems and pre-set accordingly. Receiver gain automation (RGA) posed a significant problem when reproducing data. Therefore, it was turned off and the receiver gain pre-set.

1.1.2 NMR methods

For **^{1}H NMR** experiments pre-saturation was used to suppress the water signal (transmitter frequency offset: 4.704 ppm) and ^{13}C decoupling to avoid C-H coupling in ManNac-^{13}C2 (^{13}C transmitter frequency offset: 21.868 ppm). To allow for a sufficiently long acquisition time and thus resolution, the power of the ^{13}C decoupling field was reduced to 625 Hz instead of the usual 4.16 kHz. ^{1}H-NMR experiments used as the sole detection method were run with 16 scans. In composite experiments, they were always run as the first measurement with only 2 scans. This gave enough

sensitivity to monitor the reactions of the sialic acid biosynthesis pathway, except the phosphorylation of ManNAc. Due to the necessity for multistep baseline correction in cytosolic extract experiments, the minimum substrate concentration was 200 µM - below this concentration, we found increasing reproducibility problems in the cytosolic extract experiments

SOFAST-HMQC for ManNAc-^{13}C2 solved the problem of peak separation. By decreasing the spectral width in the indirect dimension (^{13}C) to 90 Hz (0.6 ppm) and adjusting the transmitter-frequency-offset (centre of the region of interest) to the intended methyl group of ManNAc or the methylene of ManNAz, spectra with sufficient sensitivity and resolution could be recorded with 4 scans and 128 FIDs. Non-uniform sampling decreased the number of FIDs to 32 (25%), effectively minimising the measurement time to 1 min 40 sec. The characteristic shift of ManNAc-6p was corroborated with purchased ManNAc-6p. This was not possible for ManNAz-6p, and it could not be reliably calculated due to the inherent unpredictability of chemical shifts.

^{31}P-HMBC (HMBC for H-^{31}P correlations) yielded the first clear indication of ManNAz-6p in experiments with recombinant MNK. The measured correlations in the ^{31}P-HMBC of ManNAc-6p and ManNAz-6p were expected to share high chemical shift and peak shape resemblance. Recording took 1 min 26 sec at a spectral width in the indirect dimension (^{31}P) of 10 000 Hz (41.16 ppm) recorded using 4 scans and 16 FIDs. Further experiments on a lyophilised sample re-dissolved in D_2O could not validate ManNAz-6p production by recombinant MNK. Repetition at higher ManNAz concentrations, with ManNAc and NAGK and in phosphate buffer are expected to give a definitive answer.

1.1.3 Data Analysis

Real-time monitoring with 1D NMR methods was achieved by stacking spectra, which creates a 2D spectrum with time as the pseudo domain. These spectra were processed as 2D spectra. Real-time monitoring with 2D NMR methods was also achieved by stacking spectra, which creates a 3D spectrum with time as the pseudo domain. In contrast to the 1D NMR approach, the spectra were pre-processed before being stacked into a prefabricated cuboidal framework using in-house scripts.

Problems with the phase or unexpectedly changing integration values were usually caused by the receiver gain automation. Therefore, receiver gain automation was deactivated. This completely eradicated initially occurring phase problems but roughly 1 of 100 spectra still showed integration value fluctuation. A cause could not be identified.

^{1}H NMR: The pseudo 2D spectra were generated from up to 32 fids using the Bruker-script “fidtoser”. Data was zerofilled to a size of 16k in f2 (the acquisition dimension). The final signal was created by integrating a fixed number of columns always using the same spectral range for the integration. These data were converted to asci format using an in-house script and plotted using GraphPad Prism 8.

SOFAST-HMQC: Each spectrum in a set of experiments was processed using strip processing to yield a data matrix of 8k x 512 points. To process the non-uniform sampling, the compressed sensing algorithm of TopSpin was used. To ensure identical scaling of the data the topspin-parameter “nc_proc” was forced to attain an identical value. Up to 32 2D spectra were then concatenated to pseudo-3D spectrum using in-house scripts. With the help of the first 2D experiment, a roughly correct pseudo-2D plane was selected. To ensure comparability, the extracted planes were the same in each experiment set (n = 3). The resulting pseudo 2D spectra were treated like the pseudo 2D spectra of ^{1}H NMR experiments.

^{31}P-HMBC: Each spectrum in a set of experiments was processed using strip processing to yield a data matrix of 512 x 512. Up to 32 spectra were treated the same way as the SOFAST-HMQC spectra, in addition a magnitude calculation in the ^{1}H dimension was performed after creating an imaginary part using a Hilbert transform. Pseudo-2D spectra and time decays were produced as with the SOFAST_HMQC.

1.2 Protein expression

1.2.1 GNE Expression

The GNE domain of human GNE/MNK was expressed according to a protocol published by the Chen Group. [1] The gene encoding the UDP-GlcNAc 2-epimerase domain with an *N*-terminal His6-tag was bought from Biocat in a pET21a(+). The plasmid was codon optimize to be expressed in Escherichia coli BL21 (DE3) cells. The transformed BL21 (DE3) cells were stored as a glycerol stock (5%). Starting from this glycerol stock an over-day culture was grown

in 5 mL LB medium with 100 mg/L ampicillin, for 8 h at 37 °C and 220 rpm. From the over day culture an overnight culture was grown in 15 mL LB medium with 100 mg L^{-1} ampicillin, at 37 °C and 220 rpm. With 3.5 mL overnight cultures 4x500 mL LB medium with 100 mg L^{-1} ampicillin in 2 L flasks were inoculated. This was grown at 37 °C and 180 rpm to OD_{600} = 1.9. Then all cultures were pooled, and 700 mL were diluted in 1.3 L LB medium with 100 mg L^{-1} ampicillin (at 4 °C). This was redistributed to four 2 L flasks (4x500 mL), grown to OD_{600} = 0.7 and induced with IPTG (50 µM). Subsequently the cells were kept for 42 h at 8 °C and 120 rpm. Then they were grown for 24 h at 16 °C and 180 rpm. The cells were harvested by centrifugation with 4000 g for 15 min at 4 °C and the cell pellet was re-suspended in resuspension buffer (50 mM Tris-HCl, pH 8.0, 500 mM NaCl). The cells were lysed by micro fluidizing at 18 kpa (Microfluidics – LM10). The cell lysate was centrifuged with 20 000 g for 25 min at 4 °C. The clarified supernatant was filtered, and the protein was purified *via* Ni-NTA chromatography on 2x 5ml His60 Ni Superflow column – (Takara/Clontech) by a Biorad-NGC™ Chromatography System utilizing resuspension buffer and elution buffer (50 mM Tris-HCl pH 8.0, 500 mM NaCl,500 mM Imidazole) in a linear gradient over 300 mL. Fractions of the protein peak were pooled and concentrated to 10 mL using a Vivaspin 20 (Sartorius) with a molecular weight cut of at 10 kDa. The sample was then re-buffered to 50 mM Tris-HCl, pH 8.0, 100 mM NaCl, 5% glycerol and 0.2 mM TCEP using a HiPrep 26/10 Desalting column (GE Healthcare) on a Biorad-NGC™ Chromatography System. Fractions containing the GNE protein were pooled. 20 mL with a concentration of about 7 mg/mL were obtained.

1.2.2 MNK Expression

The MNK domain of human GNE/MNK was expressed according to a protocol published by the Moniot Group.[2] His6-tagged human ManNAc Kinase (hMNK) expressed from a pET28a (Novagen) vector was transformed into BL21 (DE3) cells with Kanamycin (100 mg/L). Cultures were grown at 37°C to OD_{600} between 0.6-0.8 units, induced with IPTG (1 mM), and then grown at 18°C overnight. The cells were harvested by centrifugation with 4000 g for 15 min at 4 °C and the cell pellet were re-suspended in 20 mM sodium phosphate, 0.2 mM EDTA, 1 mM DTT, pH 8.0. The cells were lysed by micro fluidizing at 18 kpa (Microfluidics – LM10). The cell lysate was centrifuged with 20 000 g for 25 min at 4 °C. The lysate was purified with Pure Cube 100 Indigo Ni-Agarose beads (Cube Biotech). First, they were washed with 200 mM sodium phosphate, pH 8, 20 mM Imidazol. MNK was eluted using 200 mM sodium phosphate and 500 mM Imidazol. Finally, MNK was rebuffered *via* a HiPrep 26/10 Desalting column (GE Healthcare) on a Biorad-NGC™ Chromatography System with buffer containing 20 mM sodium phosphate at pH 8.

1.2.3 NAGK Expression

NAGK was expressed according to a protocol published by Park Group.[3] NAGK was cloned into pET-21a vector and expressed in E.coli BL21 (DE3). Cultures were grown at 37°C to OD_{600} between 0.6-0.8 units, induced with IPTG (1 mM), and then grown at 18°C overnight. The cells were harvested by centrifugation at 4000 g, re-suspended in lysis buffer (50 mM Tris-HCl, 150 mM NaCl, 50 mM Imidazole, pH 7.5), any lysed by the microfluidizer. After the cell lysate was centrifuged at 15000 x g for 20 min at 4°C, the supernatant was loaded into a Co^{2+} loaded HiTrap™ IMAC HP. The column was rinsed with lysis buffer before the addition of elution buffer (50 mM Tris-HCl, 150 mM NaCl, 500 mM Imidazole, pH 7.5). Finally, NAGK was rebuffered via PD-10 columns to 50 mM Tris/HCl, pH 8.0, 150 mM NaCl, 1 mM DTT and 5% glycerol.

1.3 Preparation of the rat liver cytosol extracts

The rat livers were frozen in liquid nitrogen and stored at -80 °C. The frozen livers were transferred into a centrifuge tube (Falcon) and 100 mM HEPES, 100 mM NaCl, pH 7.5 was added to cover the samples. The livers were shredded with the Ultra-Turrax in short frequencies (1-2 sec., 1-2 times) on ice. The homogenate was centrifuged at 40.000 x *g* for 1 h at 4 °C. The supernatant was aliquoted into 150 µL samples, frozen in liquid nitrogen and stored at -80 °C. Protein concentration was determined by the BCA assay.

1.4 Proteomics

Proteins were digestion in-solution. In brief, urea was added to reach a final concentration of 6M. Then proteins were reduced with 5 mM TCEP and alkylated with 40 mM chloroacetamide at 37°C 60 min in the dark. Protein digestion was carried out using Lys C at an enzyme-to-protein ratio of 1:75 (w/w) at 37 °C for 4h. After diluting to 2M urea, the digestion was continued with trypsin at an enzyme-to-protein ratio of 1:100 (w/w) at 37 °C and overnight.
Digestion was stopped by adding formic acid (FA) to a final concentration of 1%. Samples were desalted with C18 Sep-Pak cartridge (Waters) and quantified with Pierce colorimetric peptide assay (Thermo Fisher Scientific). Peptides were dried under speed vacuum and stored at -20 °C.
LC-MS analysis was performed using an UltiMate 3000 RSLC nano LC system coupled on-line to an Orbitrap Fusion mass spectrometer (Thermo Fisher Scientific). Reversed-phase separation was performed using a 50 cm analytical column (in-house packed with Poroshell 120 EC-C18, 2.7µm, Agilent Technologies) with a 120 min gradient. MS^1 scans were performed in the orbitrap using 120000 resolutions; MS2 scans were acquired in the ion trap with an AGC target of 10000 and maximum injection time of 35 ms, charge state 2-4 enable for MS^2.
Raw-files were analysed in Proteome Discoverer (v. 2.4.0.400) using Sequest as search engine using the following settings: MS1 accuracy: 10 ppm; MS2 accuracy: 0.6 Da; used enzyme: trypsin; max. missed cleavages: 2; max. dynamic modifications: 4; peptide mass: 350 - 5000 Da; dynamic modifications: oxidation (methionine, +15.995 Da), static modification: carbamidomethylation (cysteine, +57.021 Da),. For FDR calculation Percolator was used with a target FDR of 1%. Label free quantification was performed using apQuant.

1.5 ManNAc-2-^{13}C Synthesis

Sodium acetate-2-^{13}C (50 mg, 602 µmol, 1 eq.) was dissolved into dry 1,4-Dioxane (5 mL) under Argon. The solution was cooled with an ice bath and DCC (149 mg, 723 µmol, 1.2 eq.) and N-hydroxysuccinimid (83 mg, 723 µmol, 1.2 eq.) were added slowly. After 30 min the ice bath was removed, and the reaction was left to stir for 16 h at room temperature. The white precipitate was removed via a Büchner funnel, and the solvent was removed under reduced pressure. The colour less solid was dissolved in dry MeOH (5 mL) 5 mL. Mannosamine HCL (194 mg, 901 µmol, 1.5 eq.) and DIPEA (523 µL. 388 mg, 3 mmol, 5 eq.) were added and the solution was left to stir for 16 h at room temperature. The crude product was purified by column chromatography on silica gel (DCM/MeOH 20:1 to 10:1 to 6.66:1) to yield the desired ManNAc-2-^{13}C (35 mg, 158 µmol, 26%) as a colour less solid.
1H NMR (600 MHz, Deuterium Oxide, 300 K) δ 5.16 (d, J = 1.6 Hz 1/2H [H1α]), 5.06 (d, J = 1.6 Hz, 1/2H [H1β]), 4.49 (dd, J = 4.6, 1.7 Hz, 1/2H [H2β]), 4.36 (dd, J = 4.7, 1.6 Hz, 1/2H [H2α]), 4.09 (dd, J = 9.8, 4.7 Hz, 1/2H [H3α]), 3.94 – 3.82 (m, 4/2H [H5/6α and H3/6β]), 3.76 (p, J = 6.7 Hz, 1/2H [H4α]), 3.66 (t, J = 9.6 Hz, 1/2H [H4β]), 3.56 (t, J = 9.9 Hz, 1/2H [H5β]), 2.11 (dd, J = 128.9, 23.7 Hz, 6/2H [HAcβ and HAcα]). (Supplementary Figure 15 and Supplementary Figure 17) ^{13}C NMR (151 MHz, Deuterium Oxide, 300 K) δ 178.55, 177.62, 95.99, 95.86, 79.16, 74.98, 74.83, 71.77, 69.69, 69.42, 63.31, 63.29, 57.01, 56.15, 24.92, 24.79 (Supplementary Figure 16). HRMS (ESI): Calc. for C7^{13}CH15NO6 [M+H]+ = 222.0933; found: C7^{13}CH15NO6 [M+H]+ = 222.1122.

1.6 ATP-Glo Plate reader Assay

Measurements were conducted in the following assay buffer unless noted otherwise: HEPES (100 mM), NaCl (100 mM), BSA (0.05 %), glycerol (5%) at pH = 7.5. Carbohydrates and ATP were applied at a final concentration of 100 µM. MNK or NAGK were applied at the indicated concentrations. Substrate and enzyme stock solutions were prepared in assay buffer. Carbohydrate and ATP solutions (2-fold concentrated, 10 µL) were dispensed into a white polystyrene 384-well microplate (3574, Corning). Then MNK or NAGK (2-fold concentrated, 10 µL) were dispensed. This procedure resulted in a final reaction volume of 20 µL. The assay plates were incubated at room temperature for 1 h. ATP-Glo assay reagent (10 µL) (Promega) was dispensed into the respective wells and the plate was incubated for another 60 min at room temperature. Luminescence signals were read out with a TECAN Infinite M Plex plate reader.

2 Supplementary Figures

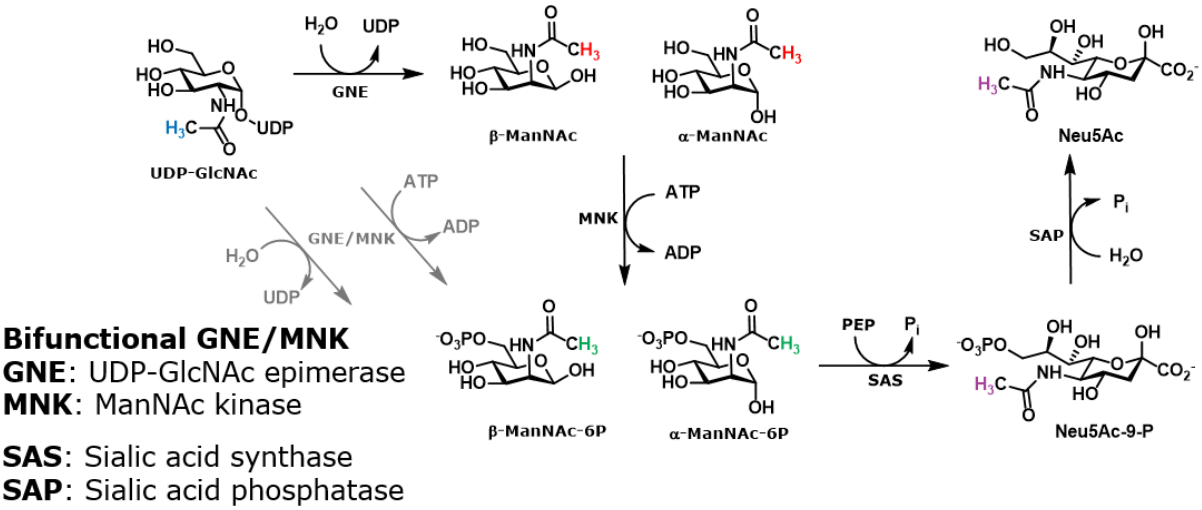

Supplementary Figure 1 - Sialic acid biosynthesis pathway scheme in which the protons of the *N*-acetyl methyl-groups are highlighted by colour code. The individual conversions with the respective enzymes are written using black font and the bifunctional GNE/MNK is highlighted with grey font.

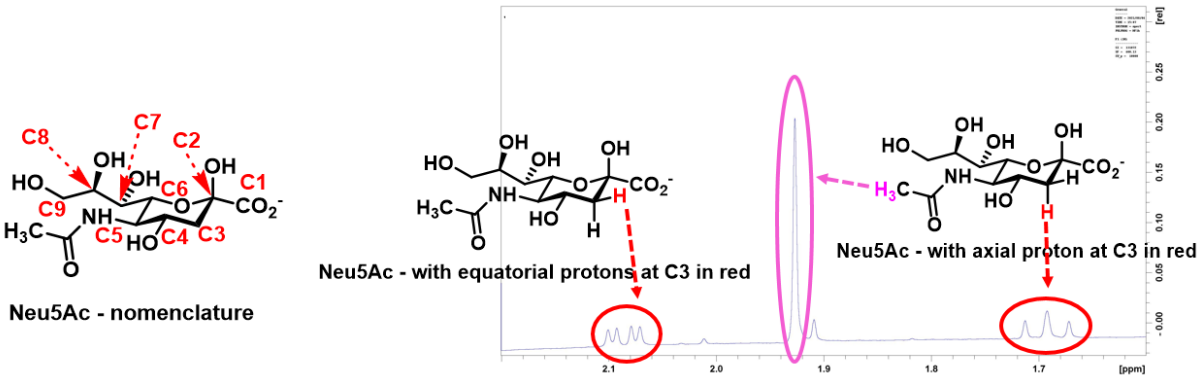

Supplementary Figure 2 - Neu5Ac signals between 2.2 and 1.6 ppm. The *N*-acetyl methyl group is a singulet. The axial proton at C3 presents as a pseudo triplet around 1.7 ppm and the equatorial proton is a doublet of doublets around 2.1 ppm.[4] This spectrum was recorded on spectrometer 2.

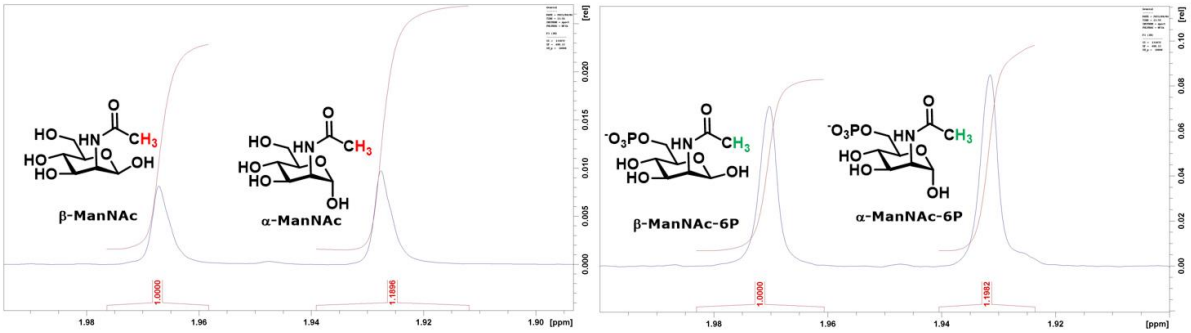

Supplementary Figure 3 – α to β ManNAc and ManNAc-6P ratio measured by the integral of the *N*-acetyl methyl groups.

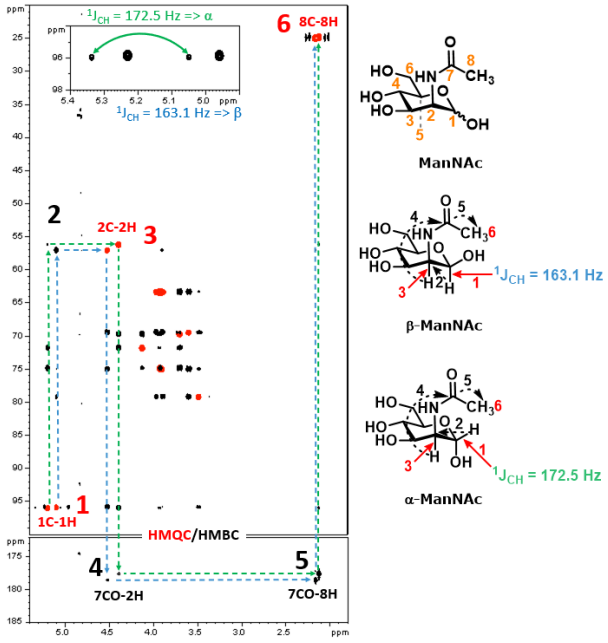

Supplementary Figure 4 - HMQC/HMBC overlay of ManNAc – the ^{1}H at the anomeric position of the β-anomer *vs.* the α-anomer has a significantly smaller coupling constant to the carbon it is bound to. Following the HMQC and HMBC signals, the *N*-acetyl groups can be assigned to their respective anomer.

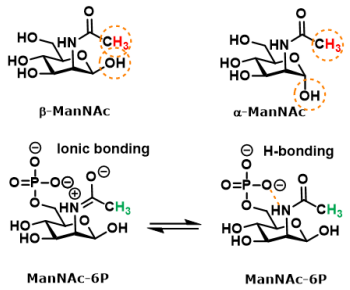

Supplementary Figure 5 - Steric interaction model of the *N*-acetyl methyl group with the anomeric hydroxyl group of ManNAc in its α and β position. Non-covalent interaction model of the phosphate of ManNAc-6P and the amide of ManNAc.

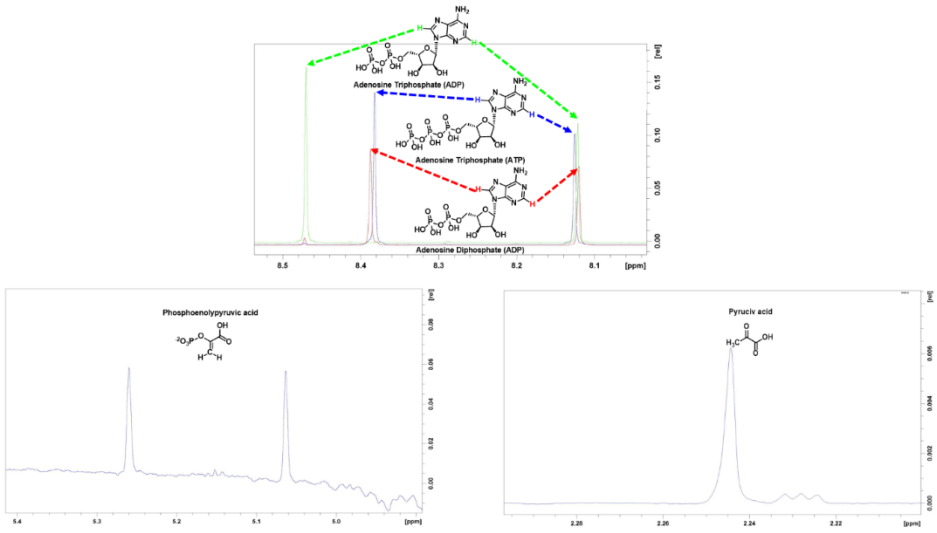

Supplementary Figure 6 – Characteristic chemical shifts of ATP, ADP, PEP and pyruvate.

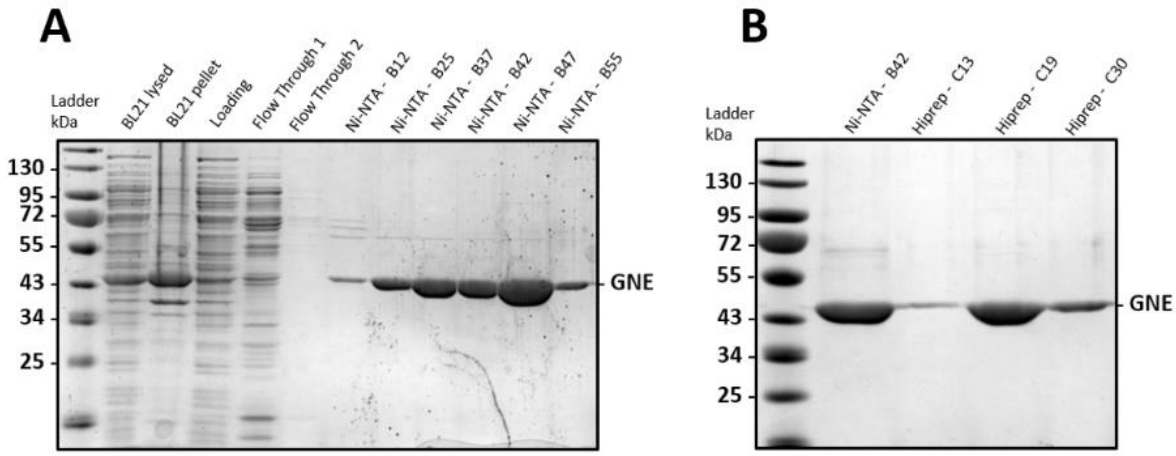

Supplementary Figure 7 – (A) SDS page (12 %) of the Ni-NTA purification of GNE. (B) SDS page (12%) of the rebuffering column conditions of GNE.

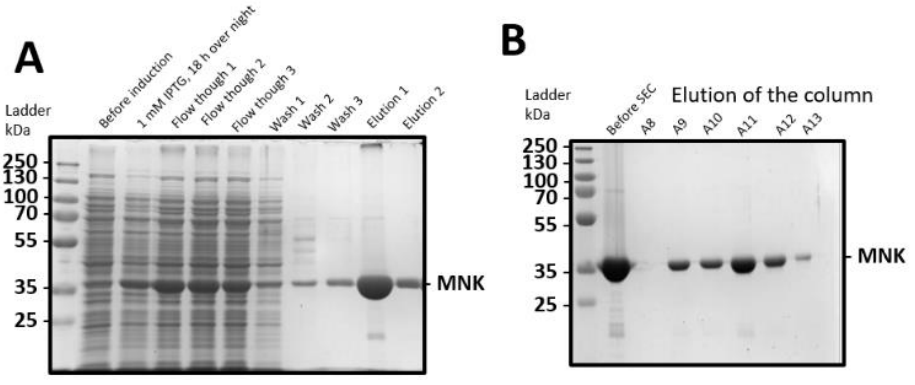

Supplementary Figure 8 – (A) SDS page (15%) of the Ni-NTA purification of MNK. (B) SDS page (15%) of the size exclusion chromatography of MNK.

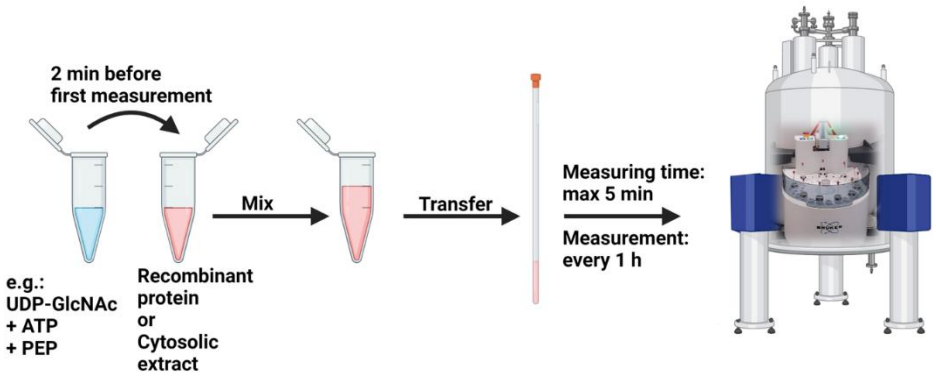

Supplementary Figure 9 - Basic experimental set for RT-NMR: 2 min before the first measurement starts, 300 µL 2x solution of substrate and cofactor were mixed with 300 µL 2x solution of recombinant proteins or cytosolic extract. The 600 µL were mixed and transferred to an NMR vial, which was placed into the autosampler of the NMR spectrometer.

$$Y = (Y0 - Plateau) * e^{(-K*X)} + Plateau$$

Supplementary Figure 10 - One-phase decay model – (Y0) Y value when X is zero; (K) rate constant

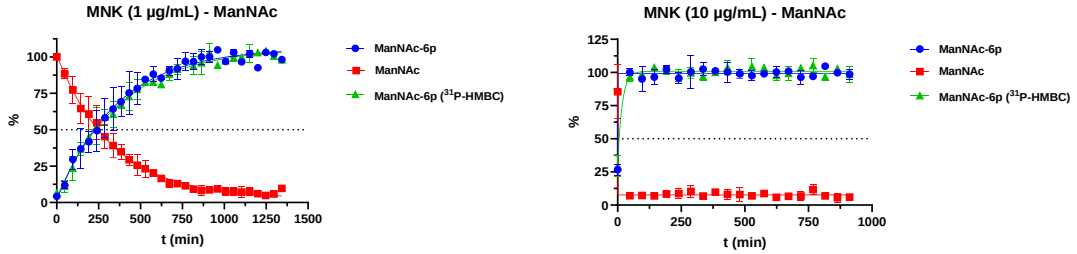

Supplementary Figure 11 – ManNAc phosphorylation at two MNK concentrations (200 µM ManNAc + 5 mM ATP).

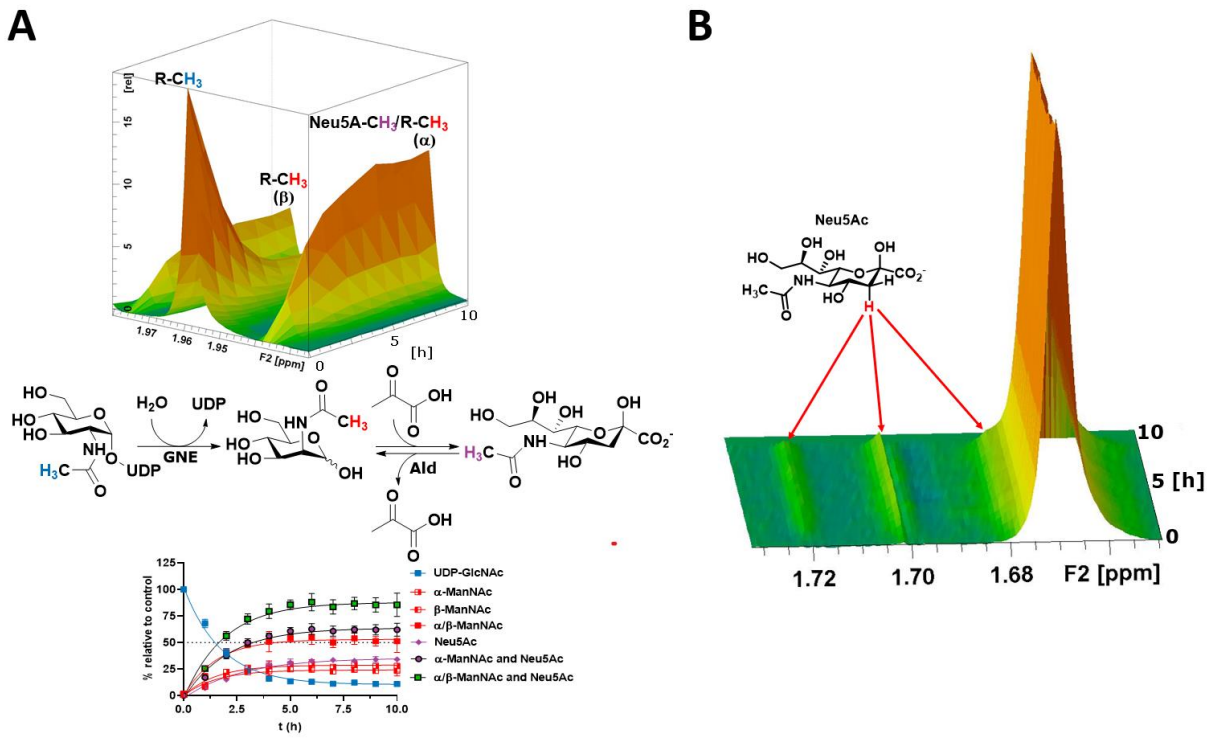

Supplementary Figure 12 – (A) Real-time ^{1}H-NMR of the conversion of UDP-GlcNAc (400 µM) to Neu5Ac by GNE (10 µg/mL) and *E. coli* sialic acid aldolase (Ald, 1 mg/mL) with pyruvate (200 mM) – nonlinear fit data in Supplementary Table 3. (B) Axial proton of Neu5Ac formation of the experiment in A.

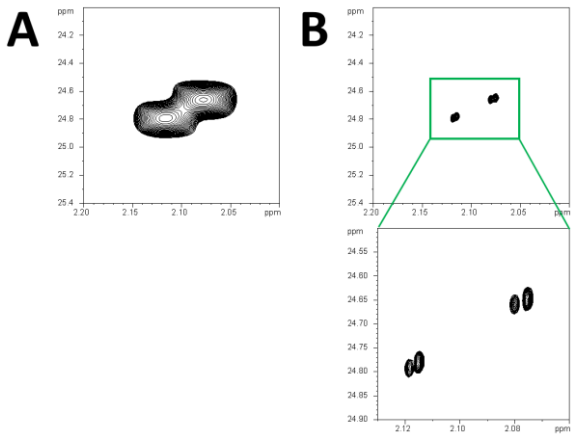

Supplementary Figure 13 - HSQC of ManNAc and ManNac-6P (1:1 – 400 µM each) (A) Normal HSQC taq (1H) = 51 msec ^{13}C-Decoupling applying B1 = 4.2 kHz taq (^{13}C) = 42 msec (B) HSQC with weak decoupling taq (1H) = 1.64 sec ^{13}C-Decoupling with B1 = 625 Hz taq (^{13}C) = 212 msec

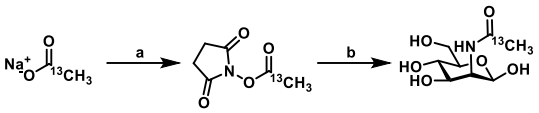

Supplementary Figure 14 – Synthesis of ManNAc-2-^{13}C. Reagents and conditions: (**a**) 1eq. sodium acetate-2-^{13}C, 1.2 eq. DCC, 1.2 eq. *N*-hydroxysuccinimid, 1,4-Dioxane, room temperature, 16 h – crude. (**b**) Crude after work up, 5 eq. DIPEA, 1.5 eq. mannosamine HCl, 16 h, room temperature, 26%.

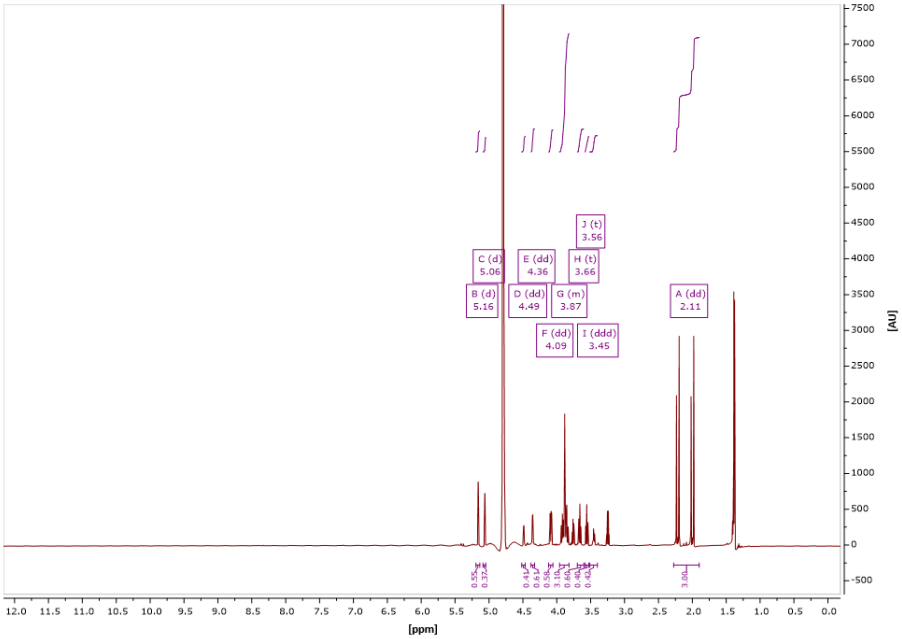

Supplementary Figure 15 – ^{1}H NMR (600 MHz) of ManNAc-2-^{13}C with minor impurities.

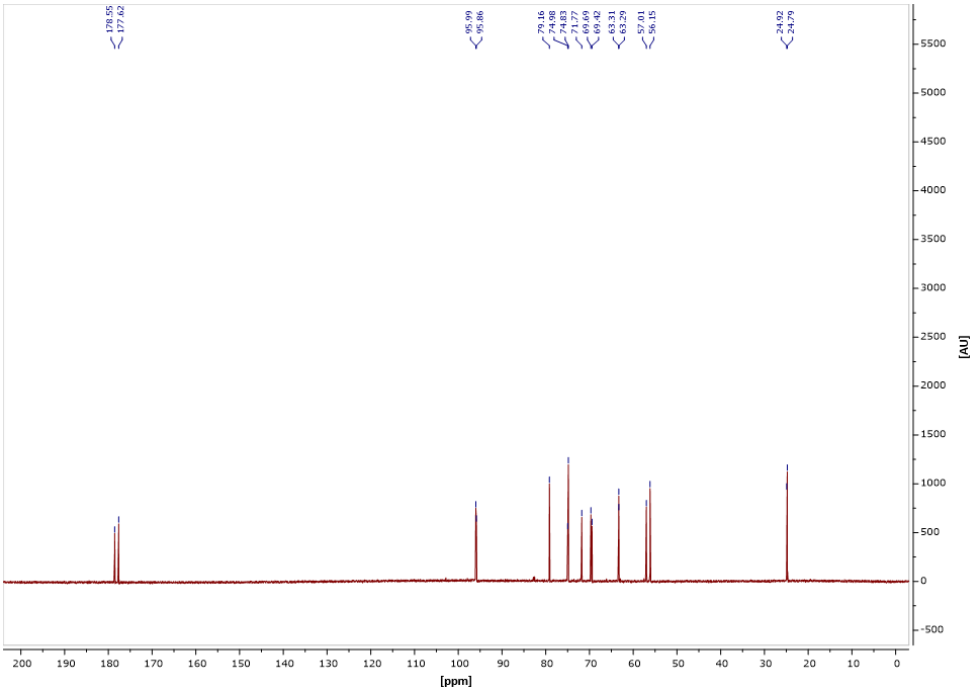

Supplementary Figure 16 – ^{13}C NMR (151 MHz) of ManNAc-2-^{13}C with minor impurities.

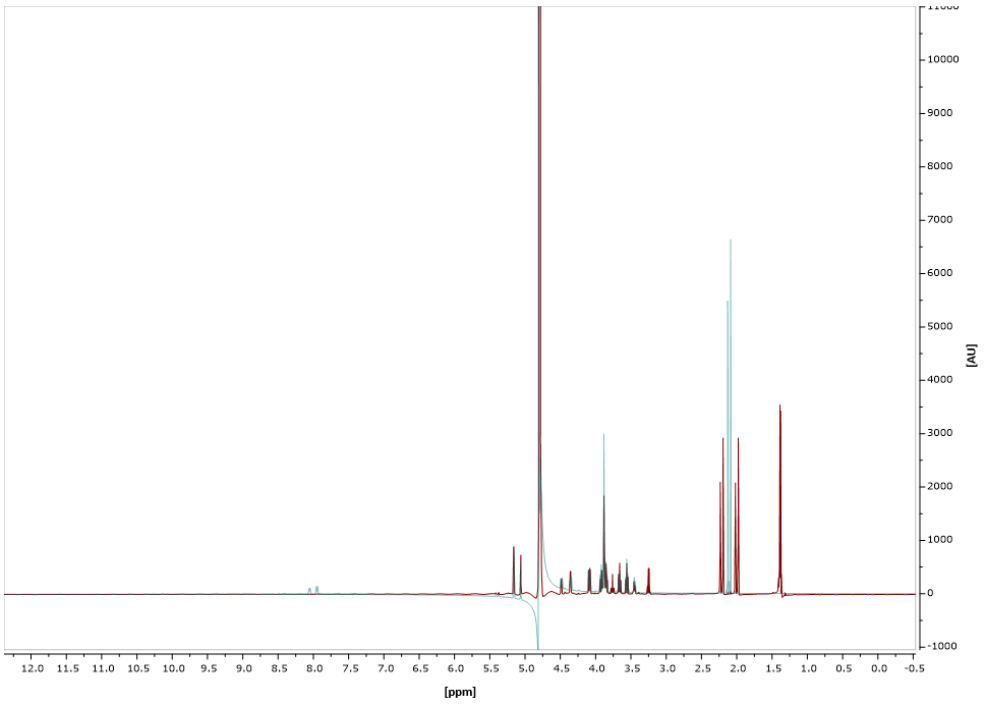

Supplementary Figure 17 – ^{1}H NMR overlay of ManNAc and ManNAc-2-^{13}C.

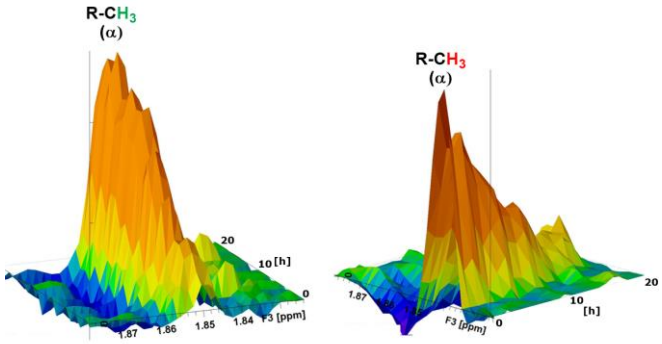

Supplementary Figure 18 - Pseudo planes of the phosphorylation of ManNAc (400 µM) to ManNAc-6p by recombinant MNK (1 µg/mL) with 5 mM ATP - α-ManNAc/-6P is marked by asteriks.

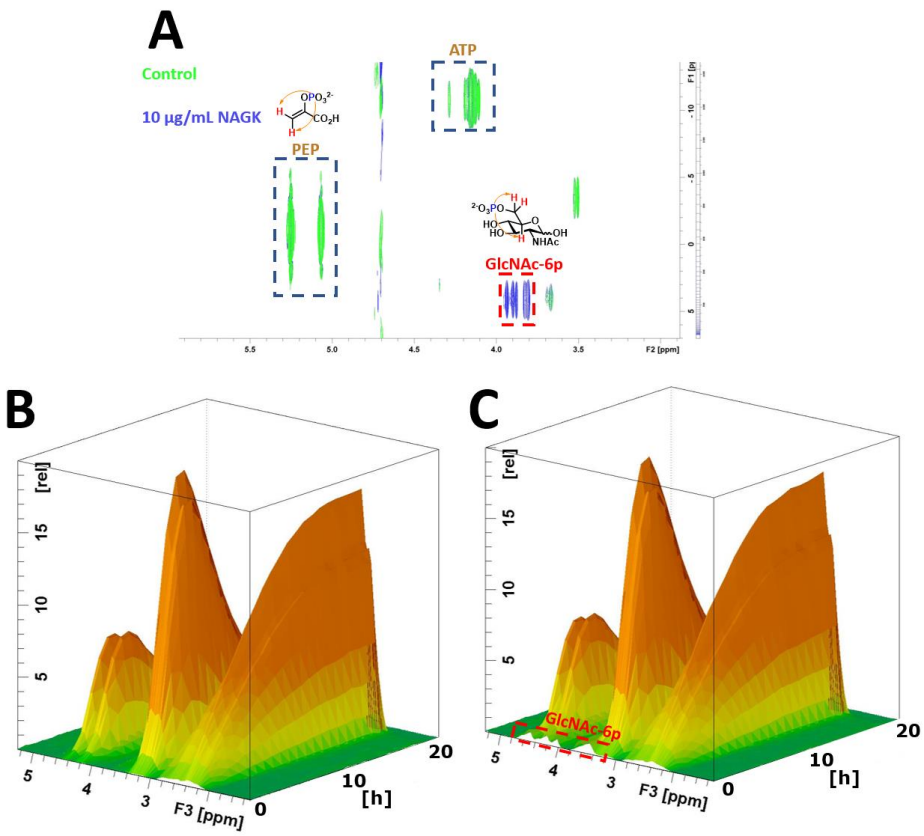

Supplementary Figure 19 – (A) Overlay of the first ^{31}P-HMBC measurement (at 0 H) of the experiments described in B and C. In this first measurement GlcNAc-6P can still be identified. In the following measurements its signal was covered by other signals. (B) RT-NMR experiment using ^{31}P-HMBC in RLCE (1.6 mg/mL) with GlcNAc (600 µM), ATP (5 mM), UTP (800 µM) and PEP (25 mM). (C) RT-NMR experiment using ^{31}P-HMBC in RLCE (1.6 mg/mL) and recombinant NAGK (10 µg/mL) with GlcNAc (600 µM), ATP (5 mM), UTP (800 µM) and PEP (25 mM).

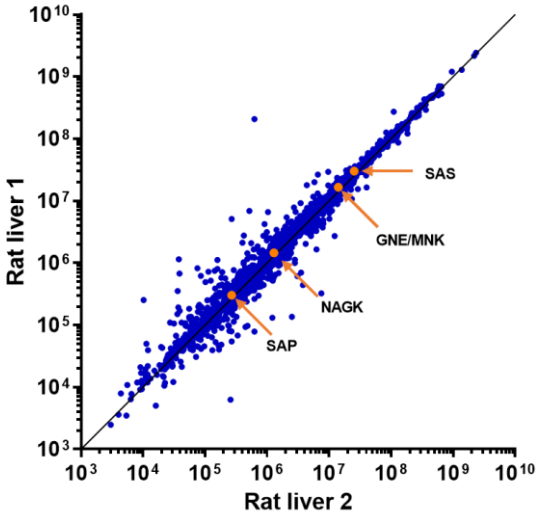

Supplementary Figure 20 – Proteomics of the rat liver cytosolic extracts used in this study. Both rat liver cytosolic extracts contain mostly the same proteins (blue). The proteins of interest are marked in orange.

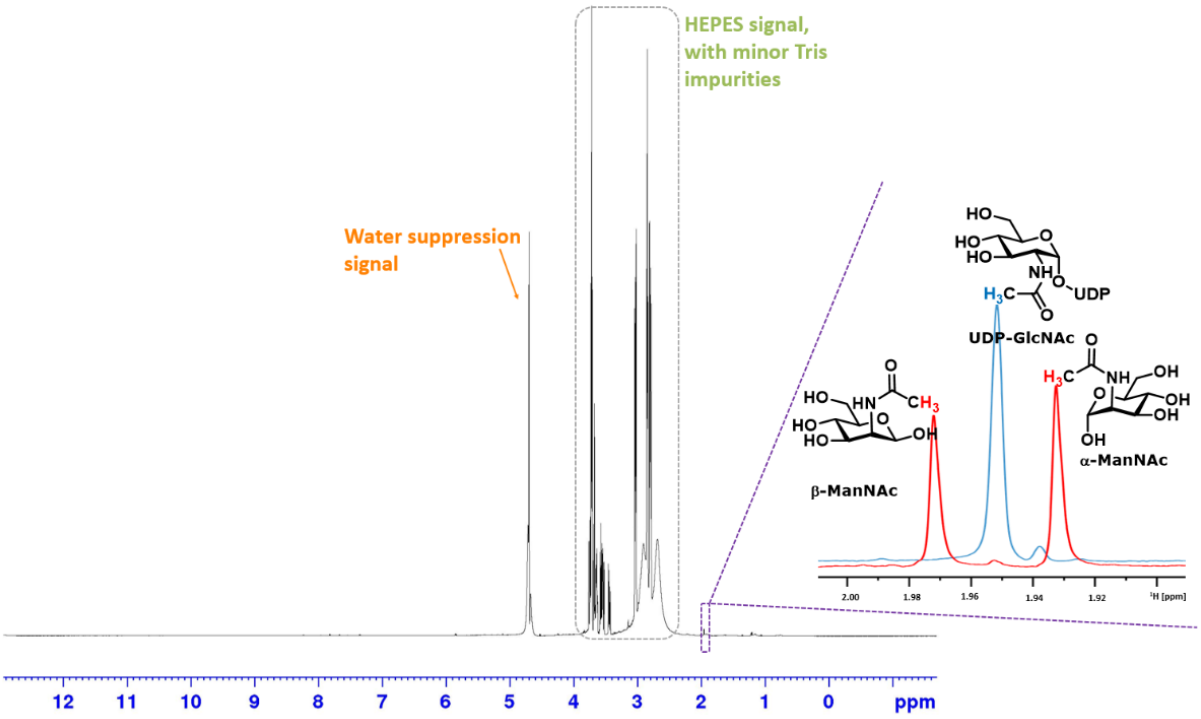

Supplementary Figure 21 – Full spectrum ^{1}H NMR (16 scans) of UDP-GlcNAc in RLCE (1.6 mg/mL). The ManNAc signals were recorded in a separate experiment and overlaid.

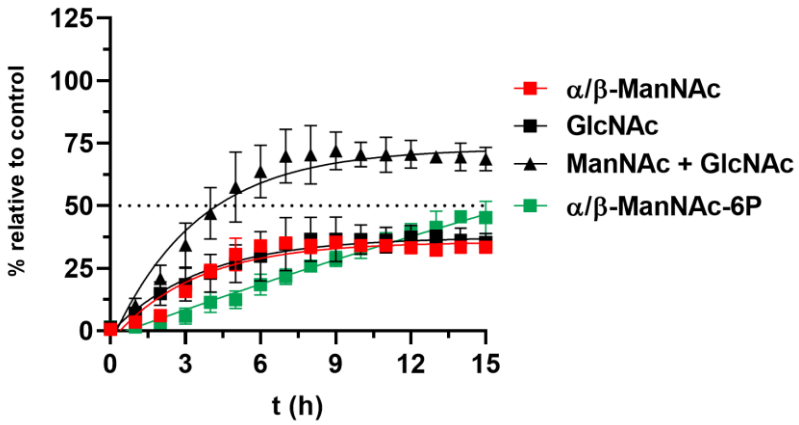

Supplementary Figure 22 – Comparison of Figure 4A (UDP-GlcNAc [400 µM] in RLCE – black and red) and Figure 4C (UDP-GlcNAc [400 µM], ATP [5 mM] and PEP [25 mM] in RLCE - green).

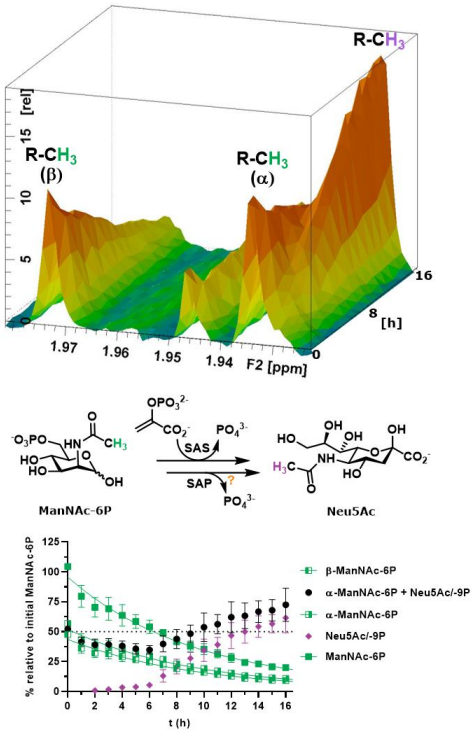

Supplementary Figure 23 - Real-time ^{1}H-NMR of the synthase reaction of ManNAc-6P (400 µM) to Neu5Ac the RLCE (6 mg/mL) with PEP (25 mM). The α-ManNAc peak is calculated relative to the β-ManNAc peak.

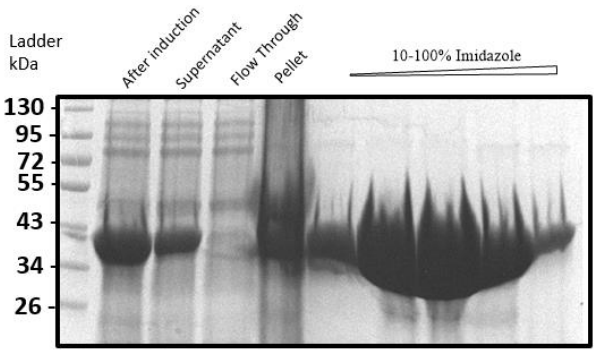

Supplementary Figure 24 – SDS page (12%) of the Ni-NTA purification of NAGK.

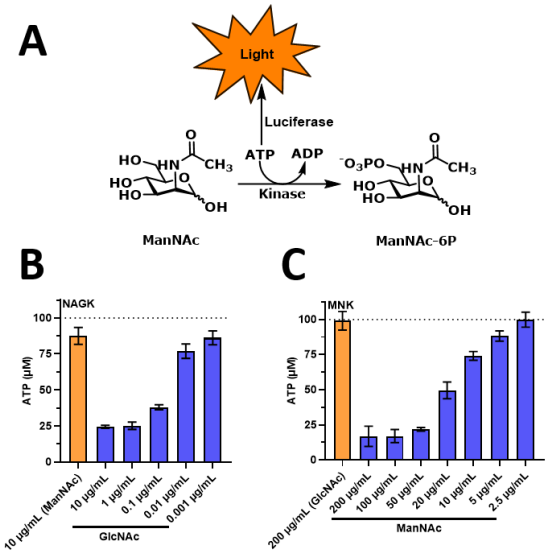

Supplementary Figure 25 – (A) Scheme depicting the principle of the ATP-Glo plate reader assay. (B-C) Results of the ATP-Glo assay with a titration of NAGK and MNK using ATP (100 µM) and ManNAc/GlcNAc (100 µM) after 1 h at room temperature. Final ATP concentration is given as calculated relative to a standard curve from 10 to 100 µM ATP.

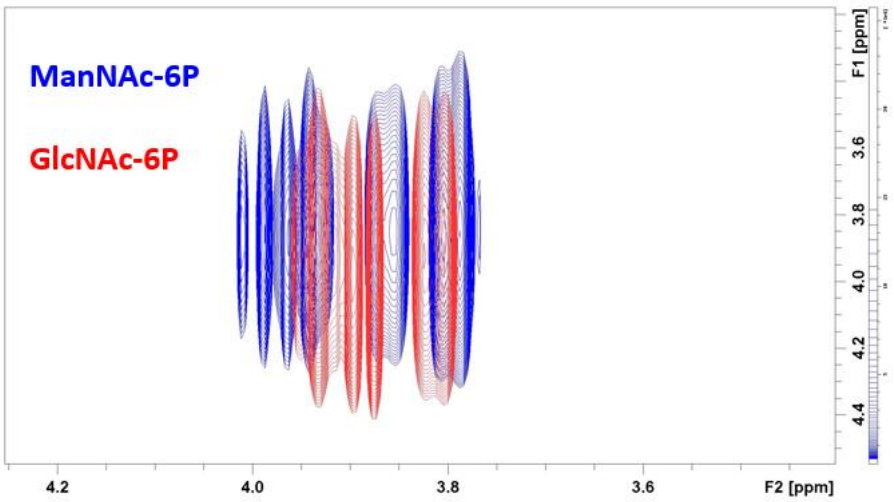

Supplementary Figure 26 – 31P-HMBC of GlcNAc-6P and ManNAc-6P.

3 Supplementary Tables

Supplementary Table 1- Nonlinear fit data for Figure 2A – One phase decay model

One phase decay

	β-ManNAc	UDP-GlcNAc	α-ManNAc	α/β-ManNAc
Best-fit values				
Y0	-0,6909	101,8	0,9141	0,2432
Plateau	47,00	0,1949	56,47	103,5
K	0,5482	0,6379	0,5888	0,5693
Half Life	1,264	1,087	1,177	1,218
Tau	1,824	1,568	1,698	1,757
Span	-47,69	101,6	-55,55	-103,2
95% CI (profile likelihood)				
Y0	-3,630 to 2,228	96,84 to 106,8	-2,463 to 4,271	-5,938 to 6,385
Plateau	45,91 to 48,13	-1,582 to 1,940	55,25 to 57,72	101,2 to 105,8
K	0,4821 to 0,6227	0,5752 to 0,7076	0,5182 to 0,6686	0,5023 to 0,6448
Half Life	1,113 to 1,438	0,9796 to 1,205	1,037 to 1,338	1,075 to 1,380
Tau	1,606 to 2,074	1,413 to 1,738	1,496 to 1,930	1,551 to 1,991
Goodness of Fit				
Degrees of Freedom	42	42	42	42
R squared	0,9620	0,9756	0,9632	0,9641
Sum of Squares	303,7	842,5	392,6	1328
Sy.x	2,689	4,479	3,057	5,624

Supplementary Table 2 - Non-linear fit data for Figure 2C – One phase decay model

One phase decay

	β-ManNAc	UDP-GlcNAc	α-ManNAc	α/β-ManNAc
Best-fit values				
Y0	0,1069	100,7	-0,5749	-0,4671
Plateau	45,49	0,2620	55,26	100,8
K	0,5342	0,6986	0,5541	0,5451
Half Life	1,297	0,9922	1,251	1,272
Tau	1,872	1,431	1,805	1,834
Span	-45,39	100,5	-55,84	-101,2
95% CI (profile likelihood)				
Y0	-2,615 to 2,810	96,68 to 104,8	-3,845 to 2,674	-6,402 to 5,429
Plateau	44,45 to 46,58	-1,158 to 1,664	54,02 to 56,53	98,49 to 103,1
K	0,4702 to 0,6062	0,6398 to 0,7632	0,4895 to 0,6267	0,4814 to 0,6167
Half Life	1,143 to 1,474	0,9082 to 1,083	1,106 to 1,416	1,124 to 1,440
Tau	1,650 to 2,127	1,310 to 1,563	1,596 to 2,043	1,622 to 2,077
Goodness of Fit				
Degrees of Freedom	41	41	41	41
R squared	0,9649	0,9836	0,9664	0,9664
Sum of Squares	253,1	534,4	362,9	1200
Sy.x	2,485	3,610	2,975	5,409

Supplementary Table 3 - Nonlinear fit data for Supplementary Figure 12 – One phase decay model

One phase decay

	β-ManNAc	UDP-GlcNAc	α-ManNAc and Neu5Ac	Neu5Ac	α/β-ManNAc	α-ManNAc	α/β-ManNAc and Neu5Ac
Best-fit values							
Y0	-0,2114	102,5	-2,561	-2,533	-0,4630	-0,2516	-2,733
Plateau	24,21	10,38	63,74	35,47	53,02	28,81	87,79
K	0,6636	0,5749	0,4834	0,3753	0,6636	0,6636	0,5278
Half Life	1,044	1,206	1,434	1,847	1,044	1,044	1,313
Tau	1,507	1,739	2,068	2,664	1,507	1,507	1,895
Span	-24,42	92,09	-66,31	-38,00	-53,49	-29,06	-90,52
95% CI (profile likelihood)							
Y0	-3,060 to 2,611	99,25 to 105,7	-6,826 to 1,670	-4,918 to -0,1736	-6,702 to 5,718	-3,642 to 3,107	-9,503 to 3,978
Plateau	23,24 to 25,21	9,173 to 11,57	62,04 to 65,53	34,32 to 36,71	50,91 to 55,21	27,66 to 30,00	85,22 to 90,46
K	0,5260 to 0,8381	0,5342 to 0,6186	0,4221 to 0,5522	0,3252 to 0,4306	0,5260 to 0,8381	0,5260 to 0,8381	0,4520 to 0,6148
Half Life	0,8271 to 1,318	1,121 to 1,298	1,255 to 1,642	1,610 to 2,132	0,8271 to 1,318	0,8271 to 1,318	1,127 to 1,533
Tau	1,193 to 1,901	1,617 to 1,872	1,811 to 2,369	2,322 to 3,075	1,193 to 1,901	1,193 to 1,901	1,627 to 2,212
Goodness of Fit							
Degrees of Freedom	42	42	42	42	42	42	42
R squared	0,8741	0,9873	0,9585	0,9597	0,8741	0,8741	0,9448
Sum of Squares	277,8	365,3	662,4	221,8	1333	393,4	1635
Sy.x	2,572	2,949	3,971	2,298	5,633	3,061	6,240

Supplementary Table 4 - Nonlinear fit data for Figure 3F – One phase decay model

One phase decay

	ManNAc-6p	ManNAc	ManNAc-6p (^{31}P-HMBC)
Best-fit values			
Y0	2,247	101,2	3,265
Plateau	108,3	1,823	107,1
K	0,1593	0,1751	0,1540
Half Life	4,352	3,958	4,502
Tau	6,278	5,710	6,495
Span	-106,0	99,36	-103,9
95% CI (profile likelihood)			
Y0	-4,156 to 8,504	96,70 to 105,7	-1,632 to 8,072
Plateau	102,8 to 115,3	-2,244 to 5,307	102,6 to 112,7
K	0,1309 to 0,1896	0,1531 to 0,1984	0,1315 to 0,1776
Half Life	3,656 to 5,294	3,494 to 4,527	3,902 to 5,272
Tau	5,274 to 7,638	5,041 to 6,531	5,630 to 7,607
Goodness of Fit			
Degrees of Freedom	47	47	47
R squared	0,9566	0,9754	0,9729
Sum of Squares	1907	939,0	1119
Sy.x	6,370	4,470	4,880

Supplementary Table 5 – calculation scheme for GlcNAc α-ManNAc and non-linear fit data for Figure 4A – One phase decay model

Signals that could be measured: β-ManNAc, UDP-GlcNAc and α-ManNAc + GlcNAc

Signals that were calculated: α-ManNAc, GlcNAc, ManNAc and ManNAc + GlcNAc

α-ManNAc = β-ManNAc * 1.2

GlcNAc = (α-ManNAc + GlcNAc) - α-ManNAc

ManNAc = β-ManNAc + α-ManNAc

ManNAc + GlcNAc = ManNAc + GlcNAc

One phase decay

	β-ManNAc	UDP-GlcNAc	α-ManNAc	α/β-ManNAc	α-ManNAc + GlcNAc	GlcNAc	ManNAc + GlcNAc
Best-fit values							
Y0	-1,988	104,8	-2,369	-4,357	-3,312	-0,9206	-5,310
Plateau	16,19	-0,8674	19,30	35,50	56,62	37,36	72,80
K	0,3011	0,4174	0,3011	0,3011	0,2855	0,2760	0,2892
Half Life	2,302	1,661	2,302	2,302	2,428	2,512	2,396
Tau	3,321	2,396	3,321	3,321	3,503	3,624	3,457
Span	-18,18	105,7	-21,67	-39,85	-59,93	-38,28	-78,11
95% CI (profile likelihood)							
Y0	-4,011 to -0,005766	99,14 to 110,6	-4,781 to -0,006873	-8,792 to -0,01264	-10,60 to 3,786	-6,966 to 4,910	-14,03 to 3,209
Plateau	15,27 to 17,24	-3,051 to 1,252	18,20 to 20,54	33,48 to 37,78	53,15 to 60,70	34,44 to 41,06	68,68 to 77,55
K	0,2377 to 0,3741	0,3746 to 0,4642	0,2377 to 0,3741	0,2377 to 0,3741	0,2172 to 0,3660	0,1899 to 0,3835	0,2260 to 0,3626
Half Life	1,853 to 2,916	1,493 to 1,850	1,853 to 2,916	1,853 to 2,916	1,894 to 3,192	1,807 to 3,650	1,911 to 3,067
Tau	2,673 to 4,207	2,154 to 2,669	2,673 to 4,207	2,673 to 4,207	2,732 to 4,604	2,608 to 5,266	2,757 to 4,425
Goodness of Fit							
Degrees of Freedom	33	33	33	33	33	33	33
R squared	0,9065	0,9776	0,9065	0,9065	0,8917	0,8315	0,9067
Sum of Squares	95,21	659,6	135,3	457,5	1229	840,4	1764
Sy.x	1,699	4,471	2,025	3,723	6,103	5,046	7,311

Supplementary Table 6 - Nonlinear fit data for Figure 4B – One phase decay model

One phase decay

	ManNAc	ManNAc-6p	PEP
Best-fit values			
Y0	103,4	-1,618	103,7
Plateau	-1,415	100,2	-8,721
K	0,6678	0,8291	0,2345
Half Life	1,038	0,8360	2,956
Tau	1,497	1,206	4,265
Span	104,8	-101,8	112,4
95% CI (profile likelihood)			
Y0	96,52 to 110,2	-11,37 to 8,097	99,06 to 108,4
Plateau	-4,089 to 1,198	96,71 to 103,7	-13,92 to -4,306
K	0,5787 to 0,7728	0,6723 to 1,035	0,2044 to 0,2661
Half Life	0,8969 to 1,198	0,6696 to 1,031	2,604 to 3,391
Tau	1,294 to 1,728	0,9660 to 1,487	3,757 to 4,893
Goodness of Fit			
Degrees of Freedom	44	45	21
R squared	0,9510	0,8999	0,9892
Sum of Squares	2162	4375	283,6
Sy.x	7,009	9,860	3,675

Supplementary Table 7 - Nonlinear fit data for Figure 4C – One phase decay model

One phase decay

	β-ManNAc-6P	UDP-GlcNAc	α-ManNAc-6P	α/β-ManNAc-6P
Best-fit values				
Y0	-1,001	102,8	-1,298	-2,297
Plateau	88,98	-34,48	142,4	226,2
K	0,01895	0,03680	0,01363	0,01603
Half Life	36,58	18,83	50,84	43,23
Tau	52,78	27,17	73,35	62,37
Span	-89,98	137,2	-143,7	-228,5
95% CI (profile likelihood)				
Y0	-2,325 to 0,2894	99,58 to 106,0	-2,761 to 0,1113	-5,060 to 0,3918
Plateau	44,03 to ???	-260,0 to 7,528	59,93 to ???	103,8 to ???
K	??? to 0,04550	0,01143 to 0,06252	??? to 0,03814	??? to 0,04126
Half Life	15,23 to ???	11,09 to 60,65	18,17 to ???	16,80 to ???
Tau	21,98 to ???	16,00 to 87,50	26,22 to ???	24,24 to ???
Goodness of Fit				
Degrees of Freedom	51	51	51	51
R squared	0,9508	0,9588	0,9571	0,9550
Sum of Squares	159,6	877,8	199,1	703,5
Sy.x	1,769	4,149	1,976	3,714

Supplementary Table 8 - Calculation scheme for Neu5Ac production from ManNAc-6P and nonlinear fit data for Supplementary Figure 23 – One phase decay model

Signals that could be measured: β-ManNAc-6P, and α-ManNAc-6P + Neu5Ac/-9P

Signals that were calculated: α-ManNAc-6P, Neu5Ac/-9P and ManNAc-6P

α-ManNAc-6P = β-ManNAc-6P * 1.2

Neu5Ac/-9P = (α-ManNAc-6P + Neu5Ac/-9P) - α-ManNAc-6P

ManNAc-6P = β-ManNAc + α-ManNAc-6P

The α-ManNAc-6P + Neu5Ac/-9P and Neu5Ac/-9P signals do not follow a one phase decay model, therefore no curve was fitted.

One phase decay

	β-ManNAc-6p	α-ManNAc-6p	ManNAc-6p
Best-fit values			
Y0	43,64	52,01	95,65
Plateau	1,142	1,361	2,503
K	0,1072	0,1072	0,1072
Half Life	6,464	6,464	6,464
Tau	9,326	9,326	9,326
Span	42,49	50,65	93,15
95% CI (profile likelihood)			
Y0	41,33 to 46,00	49,27 to 54,84	90,59 to 100,8
Plateau	-5,254 to 5,146	-6,262 to 6,133	-11,52 to 11,28
K	0,07877 to 0,1374	0,07877 to 0,1374	0,07877 to 0,1374
Half Life	5,046 to 8,799	5,046 to 8,799	5,046 to 8,799
Tau	7,280 to 12,69	7,280 to 12,69	7,280 to 12,69
Goodness of Fit			
Degrees of Freedom	37	37	37
R squared	0,9627	0,9627	0,9627
Sum of Squares	187,6	266,5	901,2
Sy.x	2,251	2,684	4,935

Supplementary Table 9 - Nonlinear fit data for Figure 5A – One phase decay model

One phase decay

	UDP-GlcNAc	UDP-GlcNAc (+ ManNAc)
Best-fit values		
Y0	100,9	97,71
Plateau	-68,02	-86,03
K	0,06181	0,04639
Half Life	11,21	14,94
Tau	16,18	21,56
Span	168,9	183,7
95% CI (profile likelihood)		
Y0	94,98 to 106,9	89,08 to 106,7
Plateau	-234,2 to -25,00	??? to -7,283
K	0,02491 to 0,09963	??? to 0,1105
Half Life	6,958 to 27,82	6,275 to ???
Tau	10,04 to 40,14	9,052 to ???
Goodness of Fit		
Degrees of Freedom	27	27
R squared	0,9690	0,9192
Sum of Squares	868,3	1928
Sy.x	5,671	8,449

Supplementary Table 10- Nonlinear fit data for Figure 5A – One phase decay model

One phase decay

	ManNAc	ManNAc-6P	ManNAc (+ UDP-GlcNAc)	ManNAc-6P (+ UDP-GlcNAc)
Best-fit values				
Y0	106,0	-3,779	111,4	-4,787
Plateau	-2,272	99,14	-8,913	98,00
K	0,3358	0,4370	0,2774	0,4026
Half Life	2,064	1,586	2,499	1,722
Tau	2,978	2,288	3,605	2,484
Span	108,3	-102,9	120,3	-102,8
95% CI (profile likelihood)				
Y0	89,73 to 122,8	-16,95 to 9,135	99,09 to 124,0	-19,25 to 9,341
Plateau	-14,57 to 6,848	93,26 to 105,7	-20,26 to -0,3373	91,21 to 105,9
K	0,2237 to 0,4808	0,3295 to 0,5688	0,2062 to 0,3579	0,2946 to 0,5391
Half Life	1,442 to 3,099	1,219 to 2,103	1,937 to 3,362	1,286 to 2,353
Tau	2,080 to 4,470	1,758 to 3,034	2,794 to 4,850	1,855 to 3,395
Goodness of Fit				
Degrees of Freedom	24	23	25	25
R squared	0,8686	0,9136	0,9279	0,8877
Sum of Squares	4068	2293	2654	3109
Sy.x	13,02	9,985	10,30	11,15

Supplementary Table 11 - Nonlinear fit data for Figure 5C – One phase decay model

One phase decay	ManNAc	ManNAc:GlcNAc (1:2)	ManNAc:GlcNAc (1:4)	ManNAc:GlcNAc (1:6)	ManNAc:GlcNAc (1:8)	ManNAc:GlcNAc (1:10)	ManNAc:Glc (1:10)	ManNAc:GalNAc (1:10)	ManNAc:Gal (1:10)	ManNAc:Man (1:10)
Best-fit values										
Y0	105,0	102,1	101,3	106,6	107,4	97,04	107,7	106,5	105,0	105,2
Plateau	-2,392	-3,231	-6,716	-6,473	-7,572	-7,595	-0,5528	-3,288	-1,152	-2,676
K	0,6082	0,4250	0,2925	0,2458	0,2042	0,1789	0,4768	0,4978	0,5083	0,4294
Half Life	1,140	1,631	2,370	2,820	3,395	3,874	1,454	1,392	1,364	1,614
Tau	1,644	2,353	3,419	4,068	4,897	5,589	2,097	2,009	1,967	2,329
Span	107,4	105,3	108,0	113,1	115,0	104,6	108,3	109,8	106,2	107,9
Std. Error										
Y0	5,289	4,687	5,708	4,766	5,620	3,571	4,481	5,120	5,757	5,107
Plateau	1,810	1,985	3,487	3,664	5,523	4,539	1,750	1,947	2,163	2,146
K	0,06673	0,04188	0,03891	0,02896	0,03111	0,02225	0,04299	0,05041	0,05976	0,04490
Span	5,412	4,761	5,802	4,959	6,235	4,442	4,563	5,219	5,872	5,189
95% CI (profile likelihood)										
Y0	94,66 to 115,5	92,91 to 111,4	90,18 to 112,7	97,37 to 116,0	96,49 to 118,6	89,93 to 104,3	98,99 to 116,5	96,52 to 116,5	93,80 to 116,4	95,35 to 115,3
Plateau	-5,995 to 1,106	-7,235 to 0,5244	-14,31 to -0,5035	-14,40 to -0,1356	-20,76 to 1,487	-18,91 to 0,2203	-4,022 to 2,769	-7,145 to 0,4098	-5,489 to 2,973	-6,940 to 1,332
K	0,4990 to 0,7396	0,3532 to 0,5090	0,2240 to 0,3720	0,1947 to 0,3027	0,1482 to 0,2661	0,1357 to 0,2258	0,4048 to 0,5593	0,4149 to 0,5952	0,4092 to 0,6285	0,3553 to 0,5157
Half Life	0,9372 to 1,389	1,362 to 1,963	1,863 to 3,094	2,290 to 3,561	2,605 to 4,677	3,070 to 5,109	1,239 to 1,712	1,165 to 1,671	1,103 to 1,694	1,344 to 1,951
Tau	1,352 to 2,004	1,965 to 2,832	2,688 to 4,464	3,304 to 5,137	3,758 to 6,747	4,429 to 7,371	1,788 to 2,470	1,680 to 2,410	1,591 to 2,444	1,939 to 2,815
Goodness of Fit										
Degrees of Freedom	44	45	45	45	44	45	45	45	45	45
R squared	0,9066	0,9206	0,8860	0,9205	0,8914	0,9383	0,9309	0,9139	0,8871	0,9112
Sum of Squares	3992	3519	5871	4334	5808	2684	3114	4019	5056	4164
Sy.x	9,525	8,843	11,42	9,814	11,49	7,723	8,318	9,451	10,60	9,620

Supplementary Table 12 - Nonlinear fit data for Figure 5C – One phase decay model

One phase decay	ManNAc	ManNAc:GlcNAc (1:2)	ManNAc:GlcNAc (1:4)	ManNAc:GlcNAc (1:6)	ManNAc:GlcNAc (1:8)	ManNAc:GlcNAc (1:10)	ManNAc:Glc (1:10)	ManNAc:GalNAc (1:10)	ManNAc:Gal (1:10)	ManNAc:Man (1:10)
Best-fit values										
Y0	0,5266	-0,7723	0,08239	-0,5647	-0,2784	-1,470	-2,447	-0,09310	-0,6667	-2,013
Plateau	105,7	103,3	107,0	106,2	107,6	112,9	101,8	104,9	105,1	104,8
K	0,5764	0,4400	0,3265	0,2530	0,2386	0,1845	0,5113	0,5030	0,5649	0,4562
Half Life	1,202	1,575	2,123	2,740	2,906	3,757	1,356	1,378	1,227	1,519
Tau	1,735	2,273	3,063	3,952	4,192	5,420	1,956	1,988	1,770	2,192
Span	-105,1	-104,0	-107,0	-106,7	-107,8	-114,4	-104,2	-105,0	-105,7	-106,8
Std. Error										
Y0	5,752	4,544	5,145	3,535	3,474	3,831	5,385	4,220	7,105	3,837
Plateau	2,128	1,876	2,773	2,609	2,870	4,620	2,016	1,595	2,522	1,544
K	0,06907	0,04229	0,03758	0,02298	0,02223	0,02186	0,05728	0,04389	0,08218	0,03587
Span	5,905	4,619	5,211	3,656	3,676	4,629	5,493	4,303	7,264	3,904
95% CI (profile likelihood)										
Y0	-10,89 to 11,82	-9,744 to 8,084	-10,13 to 10,10	-7,639 to 6,396	-7,216 to 6,543	-9,065 to 5,978	-13,03 to 8,012	-8,437 to 8,168	-14,64 to 13,10	-9,525 to 5,427
Plateau	101,6 to 109,9	99,72 to 107,0	102,0 to 112,8	101,4 to 111,8	102,4 to 113,8	105,2 to 123,4	97,94 to 105,8	101,8 to 108,0	100,3 to 110,1	101,9 to 107,9
K	0,4629 to 0,7164	0,3683 to 0,5231	0,2609 to 0,4021	0,2104 to 0,2995	0,1976 to 0,2831	0,1446 to 0,2272	0,4184 to 0,6214	0,4284 to 0,5892	0,4385 to 0,7283	0,3967 to 0,5231
Half Life	0,9675 to 1,497	1,325 to 1,882	1,724 to 2,656	2,314 to 3,295	2,448 to 3,508	3,051 to 4,792	1,115 to 1,657	1,176 to 1,618	0,9518 to 1,581	1,325 to 1,747
Tau	1,396 to 2,160	1,912 to 2,715	2,487 to 3,832	3,339 to 4,753	3,532 to 5,061	4,401 to 6,914	1,609 to 2,390	1,697 to 2,334	1,373 to 2,281	1,912 to 2,521
Goodness of Fit										
Degrees of Freedom	42	45	45	45	44	45	45	45	45	45
R squared	0,8900	0,9234	0,9057	0,9499	0,9519	0,9414	0,8963	0,9345	0,8360	0,9470
Sum of Squares	4571	3274	4603	2362	2268	3062	4417	2724	7511	2311
Sy.x	10,43	8,530	10,11	7,246	7,180	8,248	9,907	7,780	12,92	7,166

Supplementary Table 13 - Nonlinear fit data for Figure 6A – One phase decay model

One phase decay

	0.1 µg/mL	10 µg/mL
Best-fit values		Interrupted
Y0	3,676	97,16
Plateau	101,4	26239
K	0,6382	7,096e-006
Half Life	1,086	97685
Tau	1,567	140930
Span	-97,69	-26142
95% CI (profile likelihood)		
Y0	-1,612 to 8,928	
Plateau	99,69 to 103,1	
K	0,5733 to 0,7100	
Half Life	0,9763 to 1,209	
Tau	1,408 to 1,744	
Goodness of Fit		
Degrees of Freedom	35	
R squared	0,9771	
Sum of Squares	551,1	

Supplementary Table 14 - Nonlinear fit data for Figure 6B – One phase decay model

One phase decay

	0.1 µg/mL	10 µg/mL
Best-fit values		
Y0	3,666	29,17
Plateau	108,9	101,0
K	0,1483	3,427
Half Life	4,674	0,2023
Tau	6,743	0,2918
Span	-105,2	-71,81
95% CI (profile likelihood)		
Y0	-1,753 to 8,971	23,52 to 34,82
Plateau	100,3 to 121,6	99,60 to 102,4
K	0,1142 to 0,1841	2,401 to ???
Half Life	3,764 to 6,071	??? to 0,2887
Tau	5,430 to 8,759	??? to 0,4166
Goodness of Fit		
Degrees of Freedom	35	35
R squared	0,9697	0,9473
Sum of Squares	908,3	541,4

Supplementary Table 15 - Nonlinear fit data for Figure 6C– One phase decay model

One phase decay

	GlcNAc-6P	Glc-6P	Gal-6P	GalNAc-6P	Man-6P	ManNAc-6P	ManNAz-6P
Best-fit values		Ambiguous			Ambiguous		Ambiguous
Y0	-3,418	-3,849	-0,1481	0,6885	-1,829	-1,589	-0,9487
Plateau	102,0	~ 19413	3,063	-0,5094	~ 13321	119,7	~ 16218
K	0,4801	~ 0,0001289	1,061	0,7585	~ 0,0001373	0,02602	~ 0,0001338
Half Life	1,444	~ 5378	0,6533	0,9138	~ 5049	26,64	~ 5182
Tau	2,083	~ 7759	0,9425	1,318	~ 7285	38,44	~ 7476
Span	-105,5	~ -19417	-3,211	1,198	~ -13323	-121,3	~ -16219
95% CI (profile likelihood)							
Y0	-13,01 to 6,054	???	-3,461 to 3,035	-3,133 to 3,815	???	-5,411 to 1,914	???
Plateau	98,21 to 106,1	(Very wide)	2,102 to 3,747	-1,222 to 0,4443	(Very wide)	49,35 to ???	(Very wide)
K	0,3956 to 0,5798	(Very wide)	???	???	(Very wide)	??? to 0,08472	(Very wide)
Half Life	1,195 to 1,752	(Very wide)	???	???	(Very wide)	8,182 to ???	(Very wide)
Tau	1,725 to 2,528	(Very wide)	???	???	(Very wide)	11,80 to ???	(Very wide)
Goodness of Fit							
Degrees of Freedom	27	27	27	27	27	35	35
R squared	0,9492	0,9392	0,1213	0,02049	0,8699	0,8925	0,8170
Sum of Squares	1383	226,5	146,4	143,4	279,7	607,7	767,6

Supplementary Table 16 - Nonlinear fit data for Figure 6D– One phase decay model

One phase decay

	GlcNAc-6P	ManNAc-6P	ManNAz-6P
Best-fit values			
Y0	5,509	29,17	6,806
Plateau	7,204	101,0	13,28
K	0,2749	3,427	0,04232
Half Life	2,522	0,2023	16,38
Tau	3,638	0,2918	23,63
Span	-1,696	-71,81	-6,473
95% CI (profile likelihood)			
Y0	3,818 to 6,870	23,52 to 34,82	3,412 to 8,728
Plateau	6,507 to ???	99,60 to 102,4	8,879 to ???
K	???	2,401 to ???	???
Half Life	???	??? to 0,2887	???
Tau	???	??? to 0,4166	???
Goodness of Fit			
Degrees of Freedom	35	35	35
R squared	0,1075	0,9473	0,09983
Sum of Squares	71,61	541,4	275,8

[1] S. C. Chen, C. H. Huang, S. J. Lai, C. S. Yang, T. H. Hsiao, C. H. Lin, P. K. Fu, T. P. Ko, Y. Chen, *Scientific reports* **2016**, *6*, 23274-23284.
[2] J. Martinez, L. D. Nguyen, S. Hinderlich, R. Zimmer, E. Tauberger, W. Reutter, W. Saenger, H. Fan, S. Moniot, *The Journal of biological chemistry* **2012**, *287*, 13656-13665.
[3] T. Uehara, J. T. Park, *Journal of bacteriology* **2004**, *186*, 7273-7279.
[4] E. B. Brown, W. S. Brey, W. Weltner, *Biochimica et Biophysica Acta - General Subjects* **1975**, *399*, 124-130.